IET Microwaves, Antennas & Propagation

Research Article

IET Journals
The Institution of Engineering and Technology

Transmission-type negative group delay networks using coupled line doublet structure

ISSN 1751-8725
Received on 5th June 2014
Accepted on 11th November 2014
doi: 10.1049/iet-map.2014.0351
www.ietdl.org

Girdhari Chaudhary, Yongchae Jeong ✉

Division of Electronics Engineering, IT Convergence Researcher Center, Chonbuk National University, Jeollabuk-do, Jeonju, 561-756, Republic of Korea
✉ *E-mail: ycjeong@jbnu.ac.kr*

Abstract: This study presents a novel approach to the design and implementation of transmission-type negative group delay (NGD) networks based on a coupled line doublet structure. To improve the reflection coefficients, a quarter-wavelength transmission line is connected between the input and through ports of a coupled line section. For the doublet structure, two coupled line sections are arranged in a symmetrical manner by connecting them back-to-back with the help of the quarter- wavelength through line. For the experimental demonstration, two planar NGD networks (unmatched and matched doublet NGD networks) are designed, simulated and measured at a centre frequency of 2.14 GHz. From the measurement, a group delay (GD) of −5.66 ns and signal attenuation (SA) of 18.78 dB were obtained in the case of an unmatched NGD network. Similarly, for the matched NGD case, a GD of −6.33 ns, SA of 20.69 dB and input/output return losses >29 dB were obtained at the centre frequency.

1 Introduction

In recent years, an increasing amount of research has been conducted on negative group delay (NGD) networks at microwave frequencies. In a medium of refractive index $n(\omega)$, the dispersion relation [1, 2] can be written as shown in (1)

$$k = \frac{\omega n}{c} \tag{1}$$

where ω, k and c are angular frequency, wave number and speed of light, respectively. The group velocity (v_g) known as the speed of the envelope signal [2] can be given as shown in (2)

$$v_g = \frac{c}{n + \omega \mathrm{Re}(\mathrm{d}n/\mathrm{d}\omega)} \tag{2}$$

From (1) and (2), it is inferred that if the refractive index n and its derivative with respect to ω are negative (i.e. $\mathrm{d}n/\mathrm{d}\omega < 0$), the group velocity and consequently the group delay (GD) can become negative. This can happen near the absorption line or in media with a signal attenuation (SA) where the 'anomalous' wave propagation effect can occur [1, 2]. It is possible to obtain NGD phenomena in radio frequency (RF) circuits through deliberate resistive SA. Therefore lossy bandstop structures are used to realise NGD networks in a microwave regime [3–8].

The NGD phenomena might yield the output of a wave packet preceding the input peak (time advancement) [1, 3]. However, it does not violate the causality because the initial and final transient pulses are still limited to the front velocity, which will never exceed the speed of light [1–4]. The characteristics of NGD networks have been implemented in electronic circuitry and applied to various practical applications in communication systems, such as the shortening or reducing of delay lines, efficiency enhancement of a feedforward linear amplifier, bandwidth enhancement of a feedback linear amplifier and beam-squint minimisation in phased array antenna systems [5–10].

Recently, new and interesting applications of NGD networks have been reported in the realisation of non-Foster reactive elements such as negative capacitances or inductances [11]. They have opened doors for new application fields of NGD networks, such as increasing the capacitance tuning range in a varactor diode [12], or enhancing the efficiency of a class-E power amplifier by using negative capacitance to compensate the stray capacitance of a transistor [13]. It can also be extended to electromagnetic applications such as the increasing bandwidth of an artificial magnetic conductor by loading with NGD networks as non-Foster elements [14].

Basically, NGD networks can be divided into two categories: reflection- and transmission-type networks. In the reflection-type networks, the NGD characteristics are obtained from the reflected signal of the lossy bandstop structures [15–21]. These networks have excellent input/output return loss characteristics with the expense of an extra component (such as a hybrid coupler). Similarly, in the transmission-type NGD networks, the NGD phenomena are determined from the transmitting signal of lossy bandstop structures [22–28]. These networks can be designed with excellent input/output return loss characteristics with expense of extra matching networks [22, 27, 28] which increases the number of components and the circuit size as well as the SA.

In RF/microwaves, series and parallel RLC resonators are widely used to design reflection- and transmission-types NGD networks [5–9, 15–28]. To overcome the unavailability problem of lumped elements, the NGD networks using distributed elements have also been presented in the literature [5, 6, 16–23]. The periodically loaded transmission line with RLC is also used to realise NGD networks [29, 30]. In [31], the NGD network was presented using a structure that is formed by coupling a positive to a negative index transmission line. However, this structure required a matched boundary condition in order to achieve the NGD. The doublet structure is attractive for designing bandstop filters [32, 33]. However, these conventional works only concentrated on obtaining the bandstop characteristics, and not on the NGD characteristics.

In this paper, the design of transmission-type NGD networks based on the coupled line doublet structure is presented. The GD and SA are entirely controlled by the coupling coefficients and the load resistance terminated on the isolation port of the coupled line section. A transmission line in parallel with the coupled line section (connected between the input and through port of the coupled line section) is utilised to obtain excellent reflection

coefficient characteristics, which can avoid the need for any extra matching networks in transmission-type NGD networks and thus reducing the number of components. For the experimental validation of the proposed networks, two types of distributed line NGD networks (the unmatched and matched doublet structures) were fabricated and measured.

2 Analysis of NGD networks

2.1 Unmatched symmetrical doublet structure

Fig. 1*a* shows the proposed structure of the unmatched coupled line (UCL) section. In the UCL, the coupling ports are open-circuited, whereas the isolation ports are terminated with the resistor R. The Z-parameters of the reduced 2-ports UCL sections can be found as (3), derived from 4-ports coupled lines and circuit theory [34]

$$Z'_{11} = -j\frac{Z_{0e}+Z_{0o}}{2}\cot\left(\frac{\pi f}{2f_0}\right) + \frac{\left(\frac{Z_{0e}-Z_{0o}}{2}\right)^2 \csc^2\left(\frac{\pi f}{2f_0}\right)}{R - j\frac{(Z_{0e}+Z_{0o})}{2}\cot\left(\frac{\pi f}{2f_0}\right)} \tag{3a}$$

$$Z'_{12} = Z'_{21} = -j\frac{Z_{0e}+Z_{0o}}{2}\csc\left(\frac{\pi f}{2f_0}\right) + \frac{\left(\frac{Z_{0e}-Z_{0o}}{2}\right)^2 \csc\left(\frac{\pi f}{2f_0}\right)\cot\left(\frac{\pi f}{2f_0}\right)}{R - j\frac{(Z_{0e}+Z_{0o})}{2}\cot\left(\frac{\pi f}{2f_0}\right)} \tag{3b}$$

$$Z'_{22} = -j\frac{Z_{0e}+Z_{0o}}{2}\cot\left(\frac{\pi f}{2f_0}\right) + \frac{\left(\frac{Z_{0e}-Z_{0o}}{2}\right)^2 \cot^2\left(\frac{\pi f}{2f_0}\right)}{R - j\frac{(Z_{0e}+Z_{0o})}{2}\cot\left(\frac{\pi f}{2f_0}\right)} \tag{3c}$$

where Z_0 is a port reference impedance. Here, f and f_0 are the operating and design centre frequencies, respectively. The coupling coefficient C_{eff} is related with even- and odd-mode impedances (Z_{0e} and Z_{0o}) as shown in (4)

$$Z_{0e} = Z_0\sqrt{\frac{1+C_{\text{eff}}}{1-C_{\text{eff}}}} \tag{4a}$$

$$Z_{0o} = Z_0\sqrt{\frac{1-C_{\text{eff}}}{1+C_{\text{eff}}}} \tag{4b}$$

To obtain symmetrical characteristics, an unmatched doublet structure is proposed in this work. The symmetrical doublet structure NGD network shown in Fig. 1*b* is arranged by connecting back-to-back UCLs with the through line. The electrical length of the through line is $\theta = \pi/2$ at f_0 and acts as the K-inverter. The overall $ABCD$-parameters of this circuit can be obtained by matrix multiplication as shown in (5)

$$\begin{bmatrix} A_{\text{UD}} & B_{\text{UD}} \\ C_{\text{UD}} & D_{\text{UD}} \end{bmatrix} = \begin{bmatrix} \frac{Z'_{11}}{Z'_{21}} & \frac{Z'_{11}Z'_{22}-Z'^2_{12}}{Z'_{21}} \\ \frac{1}{Z'_{21}} & \frac{Z'_{22}}{Z'_{21}} \end{bmatrix} \times \begin{bmatrix} \cos\left(\frac{\pi f}{2f_0}\right) & jZ_1\sin\left(\frac{\pi f}{2f_0}\right) \\ j\frac{1}{Z_1}\sin\left(\frac{\pi f}{2f_0}\right) & \cos\left(\frac{\pi f}{2f_0}\right) \end{bmatrix} \times \begin{bmatrix} \frac{Z'_{22}}{Z'_{21}} & \frac{Z'_{11}Z'_{22}-Z'^2_{12}}{Z'_{21}} \\ \frac{1}{Z'_{21}} & \frac{Z'_{11}}{Z'_{21}} \end{bmatrix} \tag{5}$$

where $Z_1 = 1/Y_1$ is the characteristic impedance of the through line. Therefore the transmission coefficient ($S_{21\text{UD}}$) of the proposed circuit can be found by converting $ABCD$- to S-parameters [35] as shown in (6). The subscript UD represents the unmatched doublet NGD network

$$S_{11\text{UD}} = S_{22\text{UD}} = \frac{A_{\text{UD}}Z_0 + B_{\text{UD}} - C_{\text{UD}}Z_0^2 - D_{\text{UD}}Z_0}{A_{\text{UD}}Z_0 + B_{\text{UD}} + C_{\text{UD}}Z_0^2 + D_{\text{UD}}Z_0} \tag{6a}$$

$$S_{21\text{UD}} = \frac{2Z_0}{A_{\text{UD}}Z_0 + B_{\text{UD}} + C_{\text{UD}}Z_0^2 + D_{\text{UD}}Z_0} \tag{6b}$$

The GD of the unmatched doublet NGD network shown in Fig. 1*b* can be determined as (7)

$$\tau_{\text{UD}} = -\frac{\text{d}\angle S_{21\text{UD}}}{\text{d}\omega} = \frac{\text{d}}{\text{d}\omega}\left\{\tan^{-1}\frac{\text{Im}(S_{21\text{UD}})}{\text{Re}(S_{21\text{UD}})}\right\} \tag{7}$$

Furthermore, magnitudes of S-parameters and the GD of the unmatched doublet network at $f = f_0$ can be simplified as (8)

$$S_{11\text{UD}}|_{f=f_0} = S_{22\text{UD}}|_{f=f_0} = \left|\frac{R^2Z_1^2\left(1-C_{\text{eff}}^2\right)^2 - C_{\text{eff}}^4Z_1^2Z_0^2 - R^2Z_0^2}{Z_1^2\left(R-(R-Z_0)C_{\text{eff}}^2\right)^2 + R^2Z_0^2}\right| \tag{8a}$$

$$S_{21\text{UD}}|_{f=f_0} = \frac{2R^2Z_1Z_0\left(1-C_{\text{eff}}^2\right)^2}{Z_1^2\left(R-(R-Z_0)C_{\text{eff}}^2\right)^2 + R^2Z_0^2} \tag{8b}$$

(see (8c))

For better understanding of (8b) and (8c), the calculated maximum achievable GD and SA characteristics at $f_0 = 2.14$ GHz are shown in Fig. 2 for different values of Z_1. The maximum achievable GD at f_0 changes with very small changes in C_{eff}. However, the SA is improved with decreasing Z_1. Therefore low Z_1 and loose C_{eff} are preferable to improve the SA characteristics for the same amount of maximum achievable GD at f_0.

Fig. 3 shows the simulated responses of the unmatched doublet NGD network with different values of C_{eff} at $f_0 = 2.14$ GHz. The element values of this circuit are presented in Table 1 with the maximum achievable GD of -6 ns and $Z_1 = 90\ \Omega$. As seen in this figure, the NGD bandwidth decreases as C_{eff} decreases from -8 to

$$\tau_{\text{UD}}|_{f=f_0} = -\frac{Z_0\sqrt{1-C_{\text{eff}}^2}}{2Rf_0} + \frac{\left\{RZ_0\left\{\left(Z_0\sqrt{1-C_{\text{eff}}^2}\right)(R+Z_0) + RZ_1 - C_{\text{eff}}^2Z_1(R-Z_0)\right\} + Z_1^2\left(R-(R-Z_0)C_{\text{eff}}^2\right)(R+Z_0)\left(\sqrt{1-C_{\text{eff}}^2}\right)\right\}}{2f_0\left[Z_1^2\left(R-(R-Z_0)C_{\text{eff}}^2\right)^2 + R^2Z_0^2\right]} \tag{8c}$$

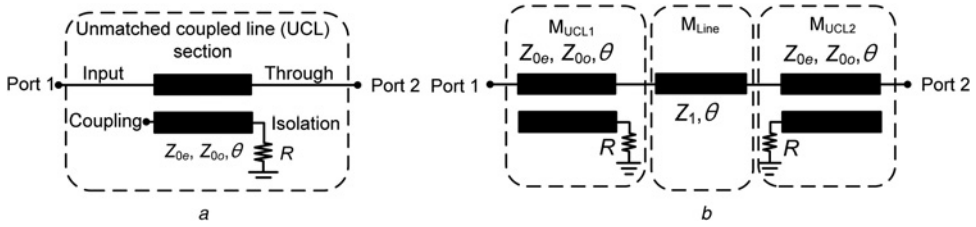

Fig. 1

a UCL section

b Configuration of the proposed unmatched doublet NGD network

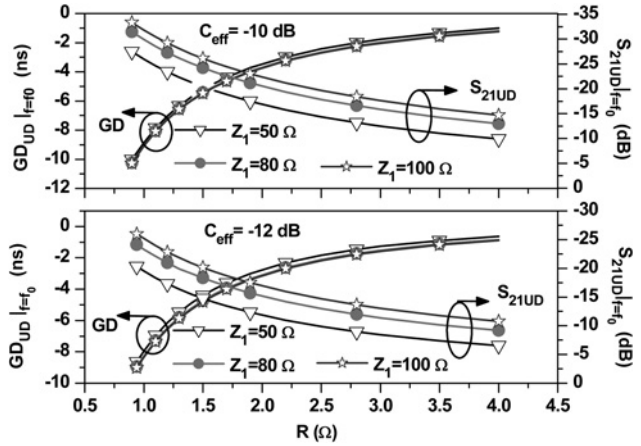

Fig. 2 *Maximum achievable NGD /magnitude characteristics of unmatched doublet NGD network at centre frequency 2.14 GHz with different values of C_{eff} and Z*

−12 dB. On the other hand, the SA of the proposed circuit is improved with the loose C_{eff}. The input/output reflection coefficients of the unmatched doublet NGD network are shown in Fig. 3 with different values of C_{eff}.

The reflection coefficients are also improved with decreasing C_{eff}. As seen in Fig. 3, the input return loss (S_{11UD}) is the same as the output return loss (S_{22UD}), which verifies that the proposed circuit is symmetrical with respect to the centre of the through line. However, the input/output impedances are not perfectly matched with the port reference impedance, and provide poor reflection characteristics. To improve the reflection characteristics of this

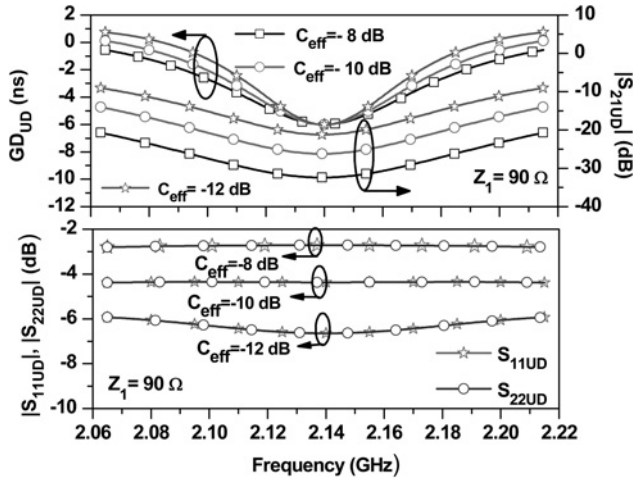

Fig. 3 *GD and S-parameter characteristics of unmatched doublet (UD) NGD network with different couplings*

Table 1 Element values of unmatched doublet NGD network with maximum achievable GD = − 6ns and Z_1 = 90 Ω for different coupling coefficients (refer to Fig. 1*b*)

C, dB	−8	−10	−12	−14
R, Ω	1.47	1.39	1.27	1.13
Z_{0e}, Ω	76.20	69.37	64.63	61.21
Z_{0o}, Ω	32.81	36.04	38.68	40.84

structure, the transmission line parallel with UCL is utilised, which is described in detail in the following section.

2.2 Matched doublet structure NGD network

Fig. 4*a* shows the matched coupled line (MCL) section. In the MCL section, the quarter-wavelength transmission line with characteristics impedance of Z_2 is connected between the input and the through ports of the coupled line section. This characteristic impedance Z_2 of parallel transmission line provides a degree of freedom to change the equivalent characteristics impedance of the coupled line structure. The *Y*-parameters of MCL can be obtained as (9)

$$Y'_{11} = \frac{Z'_{22}}{Z'_{11}Z'_{22} - Z'_{12}Z'_{21}} - \frac{j}{Z_2}\cot\left(\frac{\pi f}{2f_0}\right) \tag{9a}$$

$$Y'_{12} = Y'_{21} = -\frac{Z'_{21}}{Z'_{11}Z'_{22} - Z'_{12}Z'_{21}} + \frac{j}{Z_2}\csc\left(\frac{\pi f}{2f_0}\right) \tag{9b}$$

$$Y'_{22} = \frac{Z'_{11}}{Z'_{11}Z'_{22} - Z'_{12}Z'_{21}} - \frac{j}{Z_2}\cot\left(\frac{\pi f}{2f_0}\right) \tag{9c}$$

where Z_2 is a characteristic impedance of λ/4 line which is connected between the input and through port of the coupled line as shown in Fig. 4*a*.

Fig. 4*b* shows the structure of the matched doublet NGD network. It consists of MCL sections and a through line. The matched doublet NGD network is obtained by connecting back-to-back MCL sections with the through line, which is symmetrical with respect to the centre of the through line. The overall *ABCD*-parameters of this circuit can be obtained by matrix multiplication as shown in (10)

$$\begin{bmatrix} A_{MD} & B_{MD} \\ C_{MD} & D_{MD} \end{bmatrix} = \begin{bmatrix} \dfrac{-Y'_{22}}{Y'_{21}} & -\dfrac{1}{Y'_{21}} \\ -\dfrac{\left(Y'_{11}Y'_{22} - Y'^{2}_{12}\right)}{Y'_{21}} & \dfrac{-Y'_{11}}{Y'_{21}} \end{bmatrix}$$

$$\begin{bmatrix} \cos\left(\dfrac{\pi f}{2f_0}\right) & jZ_1\sin\left(\dfrac{\pi f}{2f_0}\right) \\ \dfrac{j}{Z_1}\sin\left(\dfrac{\pi f}{2f_0}\right) & \cos\left(\dfrac{\pi f}{2f_0}\right) \end{bmatrix} \begin{bmatrix} \dfrac{-Y'_{11}}{Y'_{21}} & -\dfrac{1}{Y'_{21}} \\ -\dfrac{\left(Y'_{11}Y'_{22} - Y'^{2}_{12}\right)}{Y'_{21}} & \dfrac{-Y'_{22}}{Y'_{21}} \end{bmatrix} \tag{10}$$

The S-parameters (S_{11MD}, S_{22MD} and S_{21MD}) of the matched doublet network can be found using ABCD- to S-parameters conversion relation [34]. For the matched doublet NGD network, the input/output reflection coefficients (S_{11MD} and S_{22MD}) should be equal to zero. Under this condition, the characteristic impedance Z_2 can be found as the fourth order polynomial shown in (11)

$$b_1 Z_2^4 - b_2 Z_2^3 - b_3 Z_2^2 - b_4 Z_2 - b_5 = 0 \tag{11}$$

where

$$b_1 = Z_0^2\left(R^2 + C_{\text{eff}}^2 Z_1^2\right) - R^2 Z_1^2\left(1 - C_{\text{eff}}^2\right) \tag{12a}$$

$$b_2 = 4Z_0 R^2 Z_1^2\left(1 - C_{\text{eff}}^2\right)^{3/2} \tag{12b}$$

$$b_3 = 6R^2 Z_0^2 Z_1^2\left(1 - C_{\text{eff}}^2\right) \tag{12c}$$

$$b_4 = 4R^2 Z_0^3 Z_1^2\left(1 - C_{\text{eff}}^2\right)^{1/2} \tag{12d}$$

$$b_5 = R^2 Z_0^4 Z_1^2 \tag{12e}$$

Therefore the required value of Z_2 is the real positive root of (11). Furthermore, the GD of this network can be determined as (13)

$$\tau_{\text{MD}} = -\frac{\text{d}\angle S_{21\text{MD}}}{\text{d}\omega} = -\frac{\text{d}}{\text{d}\omega}\left\{\tan^{-1}\frac{\text{Im}\left(S_{21\text{MD}}\right)}{\text{Re}\left(S_{21\text{MD}}\right)}\right\} \tag{13}$$

Furthermore, the magnitudes of the S-parameters and GD at $f = f_0$ can be simplified as (14)

$$S_{11\text{MD}}\big|_{f=f_0} = S_{22\text{MD}}\big|_{f=f_0} = \left|\frac{R^2 Z_0^2 Z_1^2 - C_{\text{eff}}^4 Z_1^2 Z_b^4 - R^2 Z_b^4}{Z_1^2\left(Z_b^2 C_{\text{eff}}^2 + RZ_0\right)^2 + R^2 Z_b^4}\right| \tag{14a}$$

$$S_{21\text{MD}}\big|_{f=f_0} = \frac{2R^2 Z_0 Z_1 Z_b^2}{Z_1^2\left(Z_b^2 C_{\text{eff}}^2 + RZ_0\right)^2 + R^2 Z_b^4} \tag{14b}$$

$$\tau_{\text{MD}}\big|_{f=f_0} = -\frac{Z_0\sqrt{1-C_{\text{eff}}^2}}{2Rf_0} + \frac{\left\{\begin{array}{l} RZ_b^2\left(Z_0 Z_b^2\sqrt{1-C_{\text{eff}}^2} + C_{\text{eff}}^2 Z_1 Z_b^2 + RZ_0 Z_b + RZ_0 Z_1\right) \\ + Z_1^2\left(C_{\text{eff}}^2 Z_b^2 + RZ_0\right)\left(RZ_b + C_{\text{eff}}^2 Z_0 Z_b + Z_0\sqrt{1-C_{\text{eff}}^2}\right) \end{array}\right\}}{2f_0\left\{Z_1^2\left(Z_b^2 C_{\text{eff}}^2 + RZ_0\right)^2 + R^2 Z_b^4\right\}} \tag{14c}$$

where

$$Z_b = \frac{Z_0 Z_2}{Z_2\sqrt{1-C_{\text{eff}}^2} + Z_0} \tag{15}$$

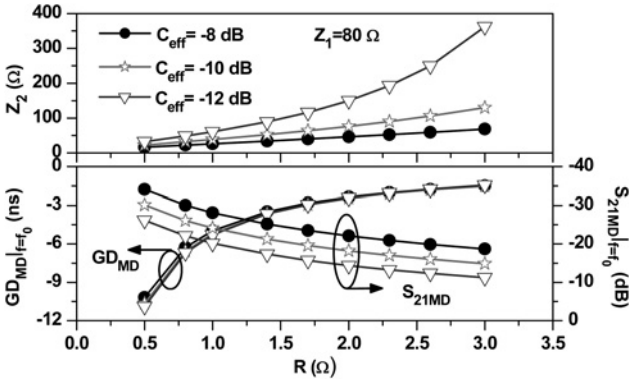

Fig. 5 *Maximum GD/magnitude characteristics of matched doublet NGD network at $f_0 = 2.14$ GHz with different value of C_{eff}*

For a better understanding of (11), (14b) and (14c), the calculated maximum achievable GD, SA and Z_2 at $f_0 = 2.14$ GHz are shown in Fig. 5 for different values of C_{eff}. The value of Z_2 will be a small when GD approaches to high value at f_0. Therefore there is a trade-off between the C_{eff}, Z_1, Z_2 and maximum NGD for the improved SA.

Fig. 6 shows the simulated response of the matched doublet NGD network with the fixed maximum achievable GD at f_0. The element values of the simulated circuit are given in Table 2 with the maximum achievable GD of -6 ns and $Z_1 = 80\ \Omega$ under different values of C_{eff}. As seen in Fig. 6 the NGD bandwidth of this circuit is almost the same for all values of C_{eff}. However, the

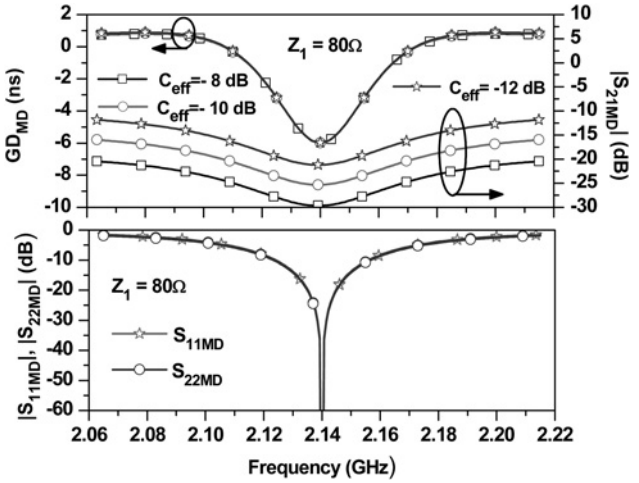

Fig. 6 *Calculated GD and S-parameters of matched doublet NGD network for different coupling coefficients*

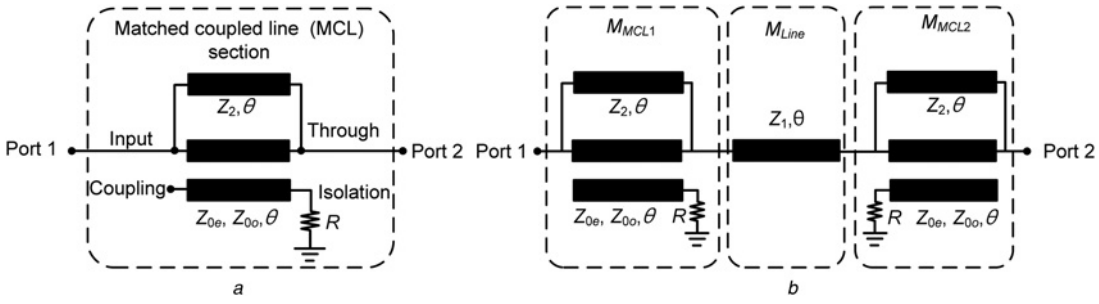

Fig. 4

a MCL section

b Configuration of the proposed matched doublet NGD network

Table 2 Element values of matched doublet structure NGD network with GD = −6 ns and $Z_1 = 80\ \Omega$ for different coupling coefficients (refer to Fig. 4*b*)

C, dB	−8	−10	−12
R, Ω	0.83	0.87	0.88
Z_2, Ω	23.05	34.35	53.51
Z_{0e}, Ω	76.20	69.37	64.63
Z_{0o}, Ω	32.81	36.04	38.68

improved SA characteristics can be obtained with decreasing C_{eff} for the fixed maximum NGD at f_0. Fig. 6 also presents the input/output return losses, which are >60 dB at f_0 and 10 dB in the range of 2.12–2.16 GHz. This response proves that the proposed matched doublet structure is symmetrical with respect to the centre of the through line.

3 Simulation and measurement results

The circuit parameters of the proposed network can be found by using parametric analysis. Therefore the design method of the proposed NGD networks is summarised as follows.

(a) First, specify the centre frequency f_0, maximum achievable GD (τ_{req}) at f_0, the characteristic impedance of the through line Z_1, and coupling coefficient C_{eff} of the coupled line.
(b) In the case of unmatched doublet NGD network, calculate the maximum achievable GD at f_0 using (8c) by assuming the value of R. Similarly, in the case of the matched doublet NGD network, calculate the value of Z_2 using (11) by assuming the value of R. After obtaining the value Z_2 for assumed R, calculate the maximum achievable GD at f_o using (14c) and (15).
(c) Compare the calculated maximum achievable GD (τ_{cal}) with the required value (τ_{req}).
(d) If $|(\tau_{\text{cal}}-\tau_{\text{req}})| \leq 0.001$ ns, R is the required value for the specified GD. If this condition is not satisfied, then change the value of R and repeat process (b) and (c).
(e) After getting final values of R and Z_2, calculate Z_{0e} and Z_{0o} using (4).
(f) Finally, obtain the width, length and spacing of the coupled line and other transmission lines according to the substrate information and optimise the physical dimensions using EM-simulator.

To verify the design concept of the doublet structure NGD networks, two types of circuits (unmatched and matched doublet NGD networks) are designed and fabricated at $f_0 = 2.14$ GHz for the GD of −6.0 ns. The networks are fabricated on a substrate RT/Duroid 5880 from Rogers Inc. with a dielectric constant (ε_r) of 2.2 and a thickness (h) of 31 mils. The simulations are performed using Ansoft's HFSS v13.

3.1 Unmatched doublet structure NGD network

For a given specification, the element values of the unmatched doublet NGD network are determined as $R = 1.14\ \Omega$, for $C_{\text{eff}} = -10$ dB and $Z_1 = 90\ \Omega$. Therefore even- and odd-mode impedances of coupled lines are determined as $Z_{0e} = 69.37\ \Omega$ and $Z_{0o} = 36.04\ \Omega$, respectively. Fig. 7 shows the EM simulation layout of an unmatched doublet NGD network with the physical dimensions, which are given in Table 3 after an optimisation. The circuit is meandered to reduce its size.

Fig. 8 shows the simulation and measurement results of the proposed unmatched doublet structure NGD network. As seen from these figures, the measurement results have good agreement with the simulations. From the experiment, the maximum achievable GD and SA of the fabricated circuit are obtained as −5.66 ns and 18.78 dB, respectively at the f_0 of 2.138 GHz. As seen in Fig. 8 the slope of the phase is positive over a certain region, which signifies the presence of NGD characteristics in the proposed circuit. A photograph of the fabricated circuit is also shown in Fig. 8.

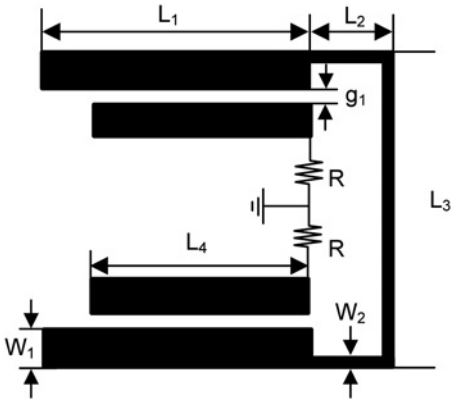

Fig. 7 *EM simulation layout of unmatched doublet NGD network with physical dimensions*

Table 3 Physical dimensions of unmatched doublet NGD network (units in millimetres) (refer to Fig. 7)

$L_1/L_2/L_3/L_4$	W_1/W_2	g_1	*R*, Ω
23.80/3.80/22.80/22.80	1.90/0.80	0.14	1.40

3.2 Matched doublet NGD network

The element values of the matched doublet NGD network are determined as $R = 0.87\ \Omega$, $Z_2 = 34.35\ \Omega$ for GD = −6 ns, $C_{\text{eff}} =$

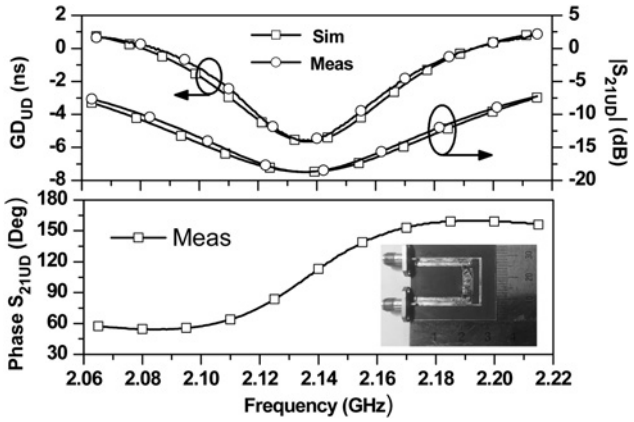

Fig. 8 *Simulation and measurement results of unmatched doublet NGD network*

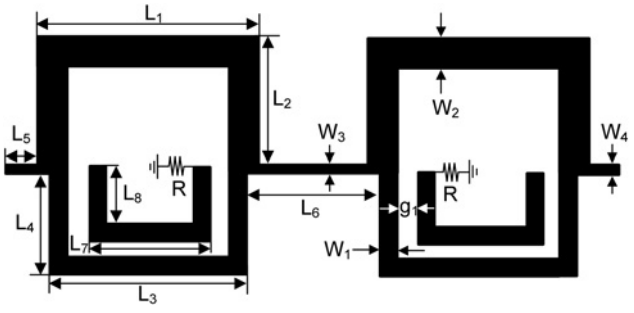

Fig. 9 *EM simulation layout of matched doublet NGD network*

IET Microw. Antennas Propag., 2015, Vol. 9, Iss. 8, pp. 748–754

Table 4 Physical dimensions of matched doublet NGD network (units in millimetres) (refer to Fig. 9)

$L_1/L_2/L_3/L_4/L_5/L_6/L_7/L_8$	$W_1/W_2/W_3/W_4$	g_1	R, Ω
17.44/12.1/16.44/9.5/1.5/24.5/12.26/6.02	1.90/2.42/1.0/1.0	0.14	0.86

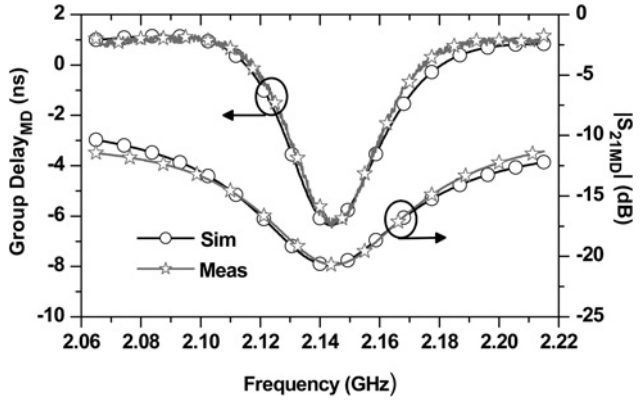

Fig. 10 *Simulation and measurement results of matched doublet NGD network*

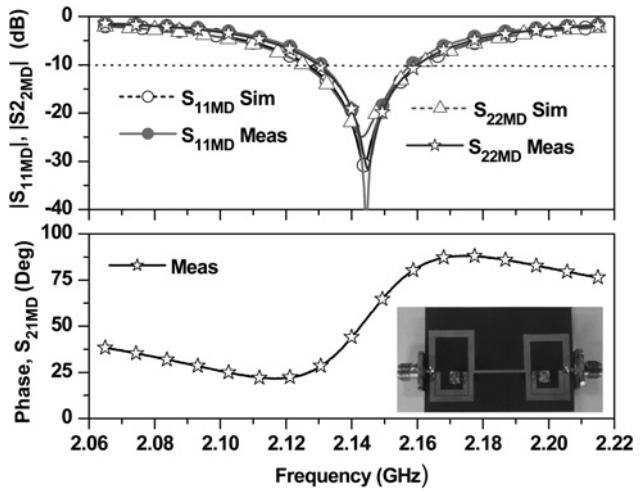

Fig. 11 *Simulated and measured S_{11}, S_{22} and transmission phase characteristics of matched doublet NGD network*

−10 dB, and $Z_1 = 80\ \Omega$. Therefore the even- and odd-mode impedances of coupled lines are determined as $Z_{0e} = 69.37\ \Omega$ and $Z_{0o} = 36.04\ \Omega$, respectively. Fig. 9 shows the EM simulation layout of the matched doublet NGD network with the physical dimensions. The overall size of the circuit is $54 \times 34\ mm^2$. After EM simulation optimisation, the dimensions of the proposed circuit are shown in Table 4.

The measurement results show good agreement with the simulations as shown in Fig. 10. From the measurement, the maximum GD and SA at the f_0 of 2.144 GHz are obtained as −6.33 ns and 20.69 dB, respectively. The input/output return losses are higher than 29 dB at the f_0 of 2.144 GHz and 15 dB for a bandwidth of 30 MHz as shown in Fig. 11. The proposed circuit provides good reflection coefficients around f_0 without the need for any extra matching circuits and so reduces the number of components (such as hybrid coupler in reflection-type NGD networks) and the overall size of circuit. The photograph of the fabricated circuit is also shown in Fig. 11. As seen in Fig. 11, the phase slope of the transmission coefficient (S_{21}) is positive in a certain frequency region and can be used for the phase compensation in communication systems such as the shifter circuit and so on.

Table 5 shows the performance of the proposed NGD networks compared with the previous works. Even though the SA of some previous transmission-type NGD circuits was compensated with the extra amplifiers, the proposed structure provides excellent return loss characteristics and moderate SA at f_0 among the transmission-type NGD networks. Therefore the proposed works do not require any extra matching networks and can be directly connected with other networks. However, the proposed NGD networks have a small NGD bandwidth. One way to increase NGD bandwidth is to cascade a number of NGD networks with slightly different operating centre frequencies [5, 6, 22]. However, it will increase SA which can be easily compensated with general purpose gain amplifiers [5, 6].

4 Conclusion

In this paper, the design and implementation of distributed transmission line NGD networks based on a coupled line doublet structure are demonstrated. The theoretical analysis shows that the NGD of the proposed structure is a function of the coupling coefficients and load resistance terminated on the isolation port of the coupled line. To obtain a symmetrical response, the doublet structure is used which consists of coupled lines connected back-to-back with the through line. A transmission line parallel to the coupled line section is utilised to provide excellent reflection coefficients, which removes the need for any extra matching

Table 5 Performance comparison of proposed NGD networks with other works

	Centre frequency f_0, GHz	Circuit type/extra matching network required	Maximum achieved NGD, ns	NGD x bandwidth product	S_{21max}, dB	Maximum return losses, dB
[5, 6]	2.14	R	−9	0.270	−63	<24
[15, 16]	1.0	R	−10	0.400	−30	X
[17, 18]	2.14	R	−5.65	0.226	−60	x
[22]	1.962	T/Y	−6.5	0.585	−21.2	<20
[23]	4.05	T/Y	−0.05	0.105	−10	x
[24]*	1.05	T/N	−2.0	0.345	0.2	12
[28]*	0.454	T/Y	−1.52	0.156	0.69	x
[29]	1.29	T/Y	−4.0	x	−28	x
[31]	0.75	T/Y	−0.5	x	x	x
This Work[1]	**2.14**	**T/Y**	**−5.66**	**0.453**	**−18.78**	**6.87**
This Work[2]	**2.14**	**T/N**	**−6.33**	**0.443**	**−20.69**	**<29.68**

T: transmission type configuration NGD network
R: reflection type configuration NGD network
Y: yes
N: no
S_{21max}: maximum Signal Attenuation at f_0
*: gain compensated NGD network
I: unmatched doublet NGD network
II: matched doublet NGD network

networks and helps to reduce the number of components and the overall size. For the experimental validation, two types of distributed transmission lines (the unmatched and matched doublet structure) of NGD networks were designed, simulated and measured at a centre frequency of 2.14 GHz. The measurement results were in good agreement with the theoretical predictions. This design method and topology are also applicable to higher order NGD networks by connecting higher numbers of the symmetric doublet structure network which can improve the NGD bandwidth and the magnitude flatness. However, this will also increase the SA. Therefore there should trade-off between NGD bandwidth and signal attenuation. The signal attenuation can be easily compensated using a general purpose gain amplifier which may decrease the overall GD. The proposed circuit can be applied in a feedforward amplifier and phased array antenna system to minimise the beam-squint.

5 Acknowledgments

This work was supported by the Basic Science Research Program through the National Research Foundation of Korea (NRF) funded by the Ministry of Education (2014R1A1A2007779).

6 References

1 Kitano, M., Nakanishi, T., Sugiyama, K.: 'Negative group delay and superluminal propagation: an electronic circuit approach', *IEEE J. Sel. Top. Quantum Electron.*, 2003, **9**, (1), pp. 43–51
2 Brillouin, L.: 'Wave propagation and group velocity' (Academic Press, New work, 1960)
3 Jeong, Y., Choi, H., Kim, C.D.: 'Experimental verification for time advancement of negative group delay in RF electronics circuits', *IET Electron. Lett.*, 2010, **46**, (4), pp. 306–307
4 Mitchell, M.W., Chia, R.Y.: 'Causality and negative group delay in a simple bandpass amplifier', *Am. J. Phys.*, 1998, **66**, (1), pp. 14–19
5 Choi, H., Jeong, Y., Kim, C.D., Kenney, J.S.: 'Efficiency enhancement of feedforward amplifiers by employing a negative group delay circuit', *IEEE Trans. Microw. Theory Tech.*, 2010, **58**, (5), pp. 1116–1125
6 Choi, H., Jeong, Y., Kim, C.D., Kenney, J.S.: 'Bandwidth enhancement of an analog feedback amplifier by employing a negative group delay circuit', *Prog. Electromagn. Res.*, 2010, **105**, pp. 253–272
7 Noto, H., Yamauchi, K., Nakayama, M., Isota, Y.: 'Negative group delay circuit for feed forward amplifier'. IEEE Int. Microwave Symp. Digest, 2007, pp. 1103–1106
8 Ravelo, B., Roy, M.L., Perennec, A.: 'Application of negative group delay active circuits to the design of broadband and constant phase shifters', *Microw. Opt. Tech. Lett.*, 2008, **50**, (12), pp. 3078–3080
9 Oh, S.S., Shafai, L.: 'Compensated circuit with characteristics of lossless double negative materials and its application to array antennas', *IET Microw. Antennas Propag.*, 2007, **1**, (1), pp. 29–38
10 Solli, D., Chiao, R.Y.: 'Superluminal effects and negative delays in electronics, and their application', *Phys. Rev. E, Stat. Phys. Plasmas Fluids Relat. Interdiscip. Top.*, 2002, **5**, pp. 0566011–05661014
11 Mirzaei, H., Eleftheriades, G.V.: 'Realizing non-Foster reactive elements using negative group delay networks', *IEEE Trans. Microw. Theory Tech.*, 2013, **61**, (12), pp. 4322–4332
12 Kolev, S., Delarcremmonniere, B., Gautier, J.L.: 'Using a negative capacitance to increase the tuning range of a varactor diode in MMIC technology', *IEEE Trans. Microw. Theory Tech.*, 2001, **49**, (12), pp. 2425–2530
13 Song, Y., Lee, S., Cho, E., Lee, J., Nam, S.: 'A CMOS class-E power amplifier with voltage stress relief and enhanced efficiency', *IEEE Trans. Microw. Theory Tech.*, 2010, **58**, (2), pp. 310–317
14 Gregoire, D.J., White, C.R., Colburn, J.S.: 'Wideband artificial magnetic conductors loaded with non-Foster negative inductors', *IEEE Antenna Wirel. Propag. Lett.*, 2011, **10**, pp. 1586–1589
15 Lucyszyn, S., Robertson, I.D.: 'Analog reflection topology building blocks for adaptive microwave signal processing applications', *IEEE Trans. Microw. Theory Tech.*, 1995, **43**, (3), pp. 601–611
16 Lucyszyn, S., Robertson, I.D., Aghvami, A.H.: 'Negative group delay synthesizer', *Electron. Lett.*, 1998, **29**, (9), pp. 798–800
17 Choi, H., Kim, Y., Jeong, Y., Kim, C.D.: 'Synthesis of reflection type negative group delay circuit using transmission line resonator'. Proc. of 39th European Microwave Conf., 2009, pp. 902–605
18 Jeong, Y., Choi, H., Kim, C.D.: 'Experimental verification for time advancement of negative group delay in RF electronics circuits', *Electron. Lett.*, 2010, **46**, (4), pp. 306–307
19 Choi, H., Kim, Y., Jeong, Y., Lim, J.: 'A design of size-reduced negative group delay circuit using a stepped impedance resonator'. Proc. of Asia-Pacific Microwave Conf., 2010, pp. 118–1121
20 Choi, H., Chaudhary, G., Moon, T., Jeong, Y., Lim, J., Kim, C.D.: 'A design of composite negative group delay circuit with lower signal attenuation for performance improvement of power amplifier linearization techniques'. IEEE Int. Microwave Symp. Digest, 2011, pp. 1–4
21 Chaudhary, G., Jeong, Y.: 'Distributed transmission line negative group delay circuit with improved signal attenuation', *IEEE Microw. Wirel. Compon. Lett.*, 2014, **24**, (1), pp. 20–22
22 Chaudhary, G., Jeong, Y., Lim, J.: 'Microstrip line negative group delay filters for microwave circuits', *IEEE Microw. Theory Tech.*, 2014, **62**, (2), pp. 234–243
23 Broomfield, C.D., Everard, J.K.A.: 'Broadband negative group delay networks for compensation of microwave oscillators and filters', *Electron. Lett.*, 2000, **9**, (23), pp. 1931–1932
24 Ravelo, B., Perennec, A., Roy, M.L., Boucher, Y.G.: 'Active microwave circuit with negative group delay', *IEEE Microw. Wirel. Compon. Lett.*, 2007, **17**, (12), pp. 861–863
25 Ravelo, B., Perennec, A., Roy, M.Le.: 'Synthesis of broadband negative group delay active circuits'. IEEE Int. Microwave Symp. Digest, 2007, pp. 2177–2180
26 Choi, H., Song, K., Kim, C.D., Jeong, Y.: 'Synthesis of negative group delay time circuit'. Proc. of Asia Pacific Microwave Conf., 2008, pp. 1–4
27 Kandic, M., Bridges, G.E.: 'Bilateral Gain-compensated negative group delay circuit', *IEEE Microw. Wirel. Compon. Lett.*, 2011, **21**, (6), pp. 308–310
28 Kandic, M., Bridges, G.E.: 'Asymptotic limit of negative group delay in active resonator-based distributed circuits', *IEEE Trans. Circuit System-I*, 2011, **58**, (8), pp. 1727–1735
29 Sidhiqui, O.F., Mojahedi, M., Eleftheriades, G.V.: 'Periodically loaded transmission line with effective negative group delay index and negative group velocity', *IEEE Trans. Antenna Propag.*, 2003, **51**, (10), pp. 2619–2625
30 Sidhiqui, O.F., Erickson, S.J., Eleftheriades, G.V., Mojahedi, M.: 'Time-domain measurement of negative group delay in negative refractive index transmission-line metamaterials', *IEEE Trans. Microw. Theory Tech.*, 2004, **52**, (5), pp. 1449–1454
31 Mirzaei, H., Islam, R., Eleftheriades, G.V.: 'Anomalous negative group velocity in coupled positive-index/negative-index guides supporting complex modes', *IEEE Trans. Antenna Propag.*, 2011, **59**, (9), pp. 3412–3420
32 Zhang, X.Y., Chan, C.H., Xue, Q., Hu, B.J.: 'RF tunable bandstop filters with constant bandwidth based on a doublet configuration', *IEEE Trans. Ind. Electron.*, 2012, **59**, (2), pp. 1257–1265
33 Levy, R., Snyder, R.V., Shin, S.: 'Bandstop filters with extended upper passbnds', *IEEE Trans. Micorw. Theory Tech.*, 2006, **54**, (6), pp. 2503–2515
34 Mathaei, G., Young, L., Jones, E.M.T.: 'Microwave filters: impedance matching networks and coupling structures' (Artech. House, Dedham, MA, 1964)
35 Pozar, D.M.: 'Microwave engineering' (John Wiley & Sons, Inc., 1998, 4th edn.)